Monolayer Exchange Chemistry of γ-Fe_2O_3 Nanoparticles

Andrew K. Boal, Kanad Das, Mark Gray, and Vincent M. Rotello*

Department of Chemistry, University of Massachusetts, Amherst, Massachusetts 01003

Received December 13, 2001. Revised Manuscript Received April 15, 2002

Monolayer modification of alkylamine-protected γ-Fe_2O_3 nanoparticles using functionalized alcohols and diols is presented. the stability of the modified nanoparticles was found to be dependent on the nature of the introduced alcohol: both bidentate surface−ligand bonding and steric blocking by bulky tail groups were necessary to produce systems resistant to agglomeration. EPR, UV−vis, and powder XRD analyses of the pre- and post-modified nanoparticles demonstrated that the core γ-Fe_2O_3 functionality was unaffected by the change in monolayer composition. Finally, multiple ligands could be readily incorporated into the monolayer using a simultaneous displacement reaction.

Introduction

Inorganic core nanoparticles coated with organic monolayers are a fundamental building block in nanotechnology.[1] The nanoscopic size of the inorganic core provides optical, magnetic, and conductive properties unique to quantum-confined materials. Uses for such systems include fluorescent biomacromolecule tags for activity assays,[2] magnetic resonance imaging (MRI) contrast agents,[3] and components for nanoscale electronic devices[4] or data storage elements.[5]

Molecular-scale properties can then be introduced into nanoparticle systems by the attachment of complex molecules to the nanoparticle surface as part of a monolayer, allowing for the creation of highly functional systems.[6] Nanoparticles functionalized with molecular recognition elements[7] add the capacity to act as selective chemical and biomacromolecular sensors,[8] building-block components in the controlled assembly of nanoparticle structures,[9] and biologically active agents.[10] One of the key aspects for the realization of the potentially powerful applications presented by the incorporation of small molecule functionality, however, is the development of divergent synthetic pathways by which such hybrid nanoparticle−monolayer systems can be created.

Numerous methods for the synthesis of nanoscopic magnetic particles, including Co-,[11] Ni-,[12] Fe-,[13] and alloy-based[14] materials have been developed. The preparation of iron oxide nanoparticles is a prevalent example of matrix-free nanoparticle synthesis and most com-

* To whom correspondence should be addressed.

(1) Shipway, A. N.; Katz, E.; Willner, I. *ChemPhysChem* **2000**, *1*, 18−52.

(2) (a) Bruchez, M., Jr.; Moronne, M.; Gin, P.; Weiss, S.; Alivisatos, A. P. *Science* **1998**, *281*, 2013−2016. (b) Chan, W. C. W.; Nie, S. *Science* **1998**, *281*, 2016−2018.

(3) (a) Shen, T. T.; Bogdanov, A., Jr.; Bogdanove, A.; Poss, K.; Brady, T. J.; Weissleder, R. *Bioconjugate Chem.* **1996**, *7*, 311−316. (b) Högemann, D.; Josephson, L.; Weissleder, R.; Basilion, J. P. *Bioconjugate Chem.* **2000**, *11*, 941−946. (c) Josephson, L.; Perez, J. M.; Weissleder, R. *Angew. Chem., Int. Ed. Engl.* **2001**, *40*, 3204−3206.

(4) Murray, C. B.; Kagan, C. R.; Wendi, M. G. *Science* **1995**, *270*, 1335−1338.

(5) (a) Black, C. T.; Murray, C. B.; Sandstrom, R. L.; Sun, S. H. *Science* **2000**, *290*, 1131−1134. (b) Pileni, M. P. *J. Phys. Chem. B* **2001**, *105*, 3358−3371.

(6) (a) Brust, M.; Walker, M.; Bethell, D.; Schiffrin, D. J.; Whymann, R. *J. Chem. Soc., Chem. Commun.* **1994**, 801−802. (b) Brousseau, L. C., III; Zhao, Q.; Shultz, D. A.; Feldheim, D. L. *J. Am. Chem. Soc.* **1998**, *120*, 7645−7646. (c) Li, H.; Luk, Y.-Y.; Mrkish, M. *Langmuir* **1999**, *15*, 4957−4959.

(7) (a) Marguerettaz, X.; Merrins, A.; Fitzmaurice, D. *J. Mater. Chem.* **1998**, *8*, 2157−2164. (b) Liu, J.; Xu, R.; Kaifer, A. E. *Langmuir* **1998**, *14*, 7337−7339. (c) Fitzmaurice, D.; Rao, S. N.; Preece, J. A.; Stoddart, J. F.; Wenger, S.; Zaccheroni, N. *Angew. Chem., Int. Ed. Engl.* **1999**, *38*, 1147−1150. (d) Boal, A. K.; Rotello, V. M. *J. Am. Chem. Soc.* **1999**, *121*, 4941−4942. (e) Aherne, D.; Rao, S. N.; Fitzmaurice, D. *J. Phys. Chem. B* **1999**, *103*, 1821−1825. (f) Boal, A. K.; Rotello, V. M. *J. Am. Chem. Soc.* **2000**, *122*, 734−735. (g) Labande, A.; Astruc, D. *Chem. Commun.* **2000**, 1007−1008. (h) Liu, J.; Alvarez, J.; Kaifer, A. E. *Adv. Mater.* **2000**, *12*, 1381−1383. (i) Kim, Y.; Johnson, R. C.; Hupp, J. T. *Nano Lett.* **2001**, *1*, 165−167. (j) Shipway, A. M.; Willner, I. *Acc. Chem. Res.* **2001**, *34*, 421−432.

(8) (a) Storhoff, J. J.; Elghanian, R.; Mucic, R. C.; Mirkin, C. A.; Letsinger, R. L. *J. Am. Chem. Soc.* **1998**, *120*, 1959−1964. (b) Labande, A.; Astruc, D. *Chem. Commun.* **2000**, 1007−1008. (c). Kim, Y.; Johnson, R. C.; Hupp, J. T. *Nano Lett.* **2001**, *1*, 165−167.

(9) (a) Mirkin, C. A.; Letsinger, R. L.; Mucic, R. C.; Storhoff, J. J. *Nature* **1996**, *382*, 607−609. (b) Alivisatos, A. P.; Johnsson, K. P.; Peng, X. G.; Wilson, T. E.; Loweth, C. J.; Bruchez, M. P.; Schultz, P. G. *Nature* **1996**, *382*, 609−611. (c) Cusack, L.; Rizza, R.; Gorelov, A.; Fitzmaurice, D. *Angew. Chem., Int. Ed. Engl.* **1997**, *36*, 848−851. (d) Boal, A. K.; Ilhan, F.; DeRouchey, J. E.; Thurn-Albrecht, T.; Russell, T. P.; Rotello, V. M. *Nature* **2000**, *404*, 746−748. (e) Shenton, W.; Davis, S. A.; Mann, S. *Adv. Mater.* **1999**, *11*, 449−452. (f) Galow, T. H.; Boal, A. K.; Rotello, V. M. *Adv. Mater.* **2000**, *12*, 576−576. (g) Shipway, A. N.; Lahav, M.; Gabai, R.; Willner, I. *Langmuir* **2000**, *16*, 8789−8795. (h) Ryan, D.; Rao, S. N.; Rensmo, H.; Fitzmaurice, D.; Preece, J. A.; Wegner, S.; Stoddart, J. F.; Zaccheroni, N. *J. Am. Chem. Soc.* **2000**, *122*, 6252−6257. (i) Lin, J.; Alvarez, J.; Ong, W.; Kaifer, A. E. *Nano Lett.* **2001**, *1*, 57−60. (j) Adachi, E. *Langmuir* **2001**, *17*, 3863−3870. (k) Jin, J.; Iyoda, T.; Cao, C.; Song, Y.; Jiang, L.; Li, T. J.; Zhu, D. B. *Angew. Chem., Int. Ed. Engl.* **2001**, *40*, 2135−2138.

(10) McIntosh, C. M.; Esposito, E. A., III; Boal, A. K.; Simard, J. M.; Martin, C. T.; Rotello, V. M. *J. Am. Chem. Soc.* **2001**, *123*, 7626−7629.

(11) (a) Osuna, J.; de Caro, D.; Amiens, C.; Chaudret, B.; Snoeck, E.; Respaund, M.; Broto, J.-M.; Fert, A. *J. Phys. Chem.* **1996**, *100*, 14571−14574. (b) Lin, X. M.; Sorensen, C. M.; Klabunde, K. J.; Hadjipanayis, G. C. *Langmuir* **1998**, *14*, 7140−7146.

(12) (a) Ely, T. O.; Amiens, C.; Chaudret, B.; Snoeck, E.; Verelst, M.; Respaund, M.; Broto, J.-M. *Chem. Mater* **1999**, *11*, 526−529 (b) Zach, M. P.; Penner, R. M. *Adv. Mater.* **2000**, *12*, 878−883. (c) Chen, D.-H.; Wu, S.-H. *Chem. Mater.* **2000**, *12*, 1354−1360.

(13) (a) Suslick, K. S.; Fang, M.; Hyeon, T. *J. Am. Chem. Soc.* **1996**, *118*, 11960−11961. (b) Sun, Y.-P.; Rollins, H. W.; Guduru, R. *Chem. Mater.* **1998**, *11*, 7−9.

(14) (a) Teranishi, T.; Miyake, M. *Chem. Mater.* **1999**, *11*, 3414−3416. (b) Duxin, N.; Pileni, M. P.; Wernsdorfer, W.; Barbara, B.; Mailly, D. *Langmuir* **2000**, *16*, 11−14. (c) Liu, C.; Zou, B. S.; Rondinone, A. J.; Zhang, J. *J. Am. Chem. Soc.* **2000**, *122*, 6263−6267. (d) Ngo, A.-T.; Pileni, M.-P. *Adv. Mater.* **2000**, *12*, 276−279. (e) Pithawalla, Y. B.; El-Shall, M. S.; Deevi, S. C.; Strom, V.; Rao, K. V. *J. Phys. Chem. B* **2001**, *105*, 208−2090.

10.1021/cm011689p CCC: $22.00
Published on Web 05/16/2002

monly involve a sol−gel-like hydrolysis formation process in inverse micelles, leading to water-dispersible nanoparticles.[15] A method for the production of organic-solvent-dispersible *amorphous* Fe_2O_3 or Fe nanoparticle agglomerates, based on the sonication of $Fe(CO)_5$ in alkane solvents, has also been described.[16] In terms of monolayer chemistry, these nanoparticle agglomerates are among the most extensively studied systems and have been coated with alkane thiols,[17] alcohols,[18] phosphonic, and sulfonic acids.[19] Recently, a method for the production of monolayer-coated discrete iron oxide nanoparticles has been described. In that report, the sonication of $Fe(CO)_5$ in the presence of undecenoic, dodecyl sulfonic, and octyl phosphonic acids allowed for the formation of polydisperse monolayer-coated amorphous Fe_2O_3 nanoparticles of 6−15-nm diameter.[20]

Recently, Alivisatos et al. described the preparation of soluble crystalline γ-Fe_2O_3 nanoparticles.[21] In this reaction, iron(III) cupferron (**1**) is thermally decomposed at high temperature in a mixture of trioctylamine and octylamine to yield highly monodisperse monolayer-protected iron oxide nanoparticles (MPNs), MPN **2** (Figure 1). These MPNs are soluble in a number of nonpolar organic solvents such as $CHCl_3$ and toluene and can be readily precipitated from solution with polar solvents. Because the monolayer is composed of alkylamines, these molecules should be displaced by harder Lewis base ligands such as alcohols. This system therefore presents an excellent opportunity for tuning of the monolayer functionality after the preparation of the nanoparticle core itself. Additionally, these systems are highly attractive from the applications perspective as they are nanocrystalline as opposed to amorphous iron oxide and, thus, they might be useful in the creation of magnetic data storage devices and other applications.

In the present work, we identify a ligand system capable of modifying the monolayer shell of MPN **2** to produce agglomeration-resistant nanoparticles. Further, we characterize the nature of the monolayer and explore the effects of the monolayer composition on both monolayer and core structures. Finally, we examine the exchange reaction itself, including synthetic methodologies for yielding the most extensively functionalized monolayer and establishing protocols by which multiple incoming ligands can be attached to the nanoparticle surface.

Results and Discussion

Monolayer Displacement. Our initial attempt to modify the monolayer of MPN **2** was based on the incorporation of dodecanol into the nanoparticle monolayer (Scheme 1). In this case, we dissolved both MPN **2** and a large excess of dodecanol in toluene and stirred the reaction mixture for 48 h at room temperature. After removal of the bulk of the solvent, the nanoparticles could be precipitated by the addition of a large excess of EtOH. Once precipitation was complete and the solid had been collected and rinsed, the resulting MPN could be fully resuspended in toluene or $CHCl_3$ (Figure 2a). Unlike the starting material, however, solutions of the

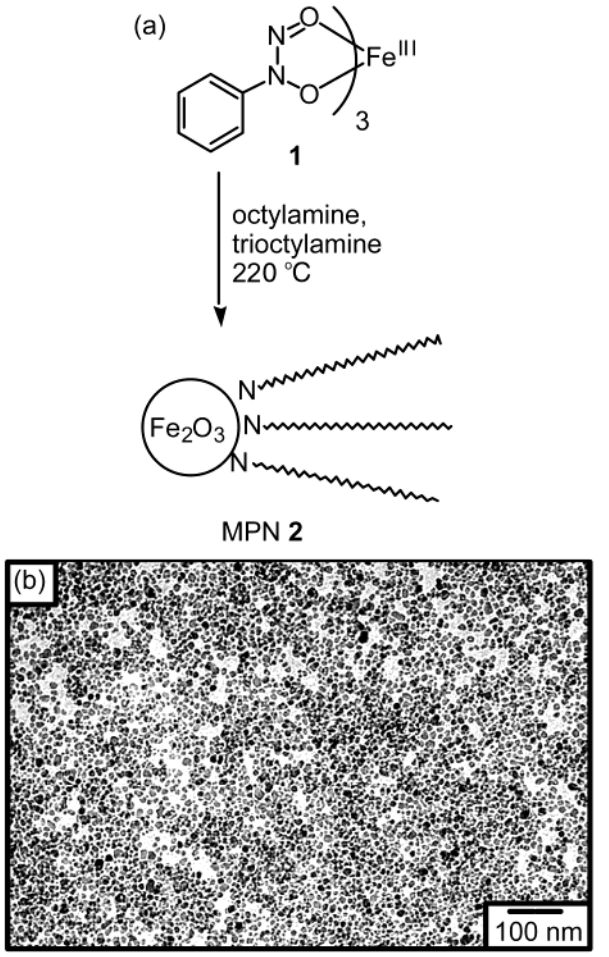

Figure 1. (a) Scheme for Alivisatos' preparation of MPN **2**[21] and (b) TEM micrograph of the as-produced nanoparticles from our laboratory.

Scheme 1. Attempted Exchange of Dodecanol into the Monolayer of MPN 2

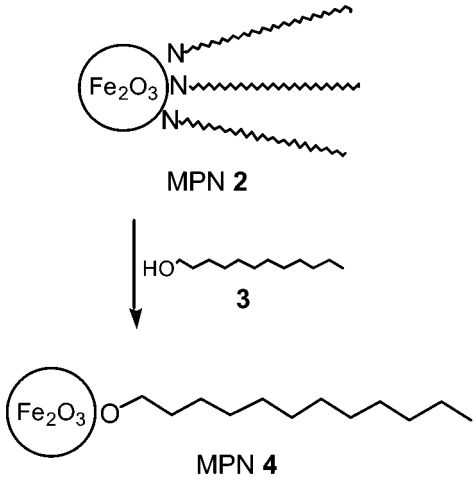

(15) (a) Pileni, M.-P. *J. Phys. Chem.* **1993**, *97*, 9661−3896. (b) Pileni, M.-P. *Langmuir* **1997**, *13*, 3266−3276.
(16) Suslick, K. S.; Hyeon, T.; Fang, M. *Chem. Mater.* **1996**, *8*, 2172−2179.
(17) Kataby, G.; Ulman, A.; Prozorov, R.; Gedanken, A. *Langmuir* **1998**, *14*, 1512−1515.
(18) Kataby, G.; Prozorov, T.; Koltypin, Y.; Cohen, H.; Sukenik, C. N.; Ulman, A.; Gedanken, A. *Langmuir* **1997**, *13*, 6151−6158.
(19) Yee, C.; Kataby, G.; Ulman, A.; Prozorov, T.; White, H.; King, A.; Rafailovich, M.; Sokolov, J.; Gedanken, A. *Langmuir* **1999**, *15*, 7111−7115.
(20) Shafi, K. V. P. M.; Ulman, A.; Yan, X.; Yang, N.-L.; Estournès, C.; White, H.; Rafailovich, M. *Langmuir* **2001**, *17*, 5093−5097.
(21) Rockenberger, J.; Scher, E.; Alivisatos, A. P. *J. Am. Chem. Soc.* **1999**, *121*, 11595−11596.

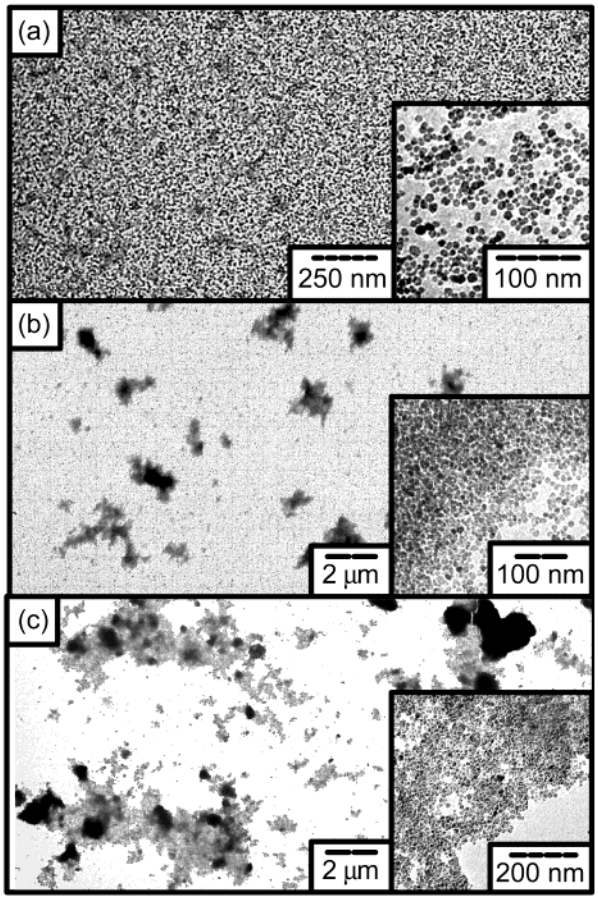

Figure 2. TEM micrographs of MPN **4** (a) immediately after purification, (b) after aggregation, and (c) after sonication of the insoluble material.

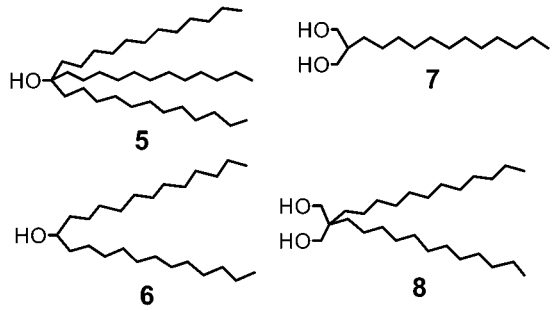

Figure 3. Alcohol ligands used in exchange reactions with MPN **2**.

MPNs slowly formed a precipitate over several days (Figure 2b), with the ultimate formation of an intractable black solid. This material could not be redissolved in any standard solvent, and a similar irreversible agglomeration was observed if the nanoparticles were dried in vacuo after precipitation from the reaction mixture. Sonication of this precipitate in $CHCl_3$ yielded cloudy gray suspensions consisting mostly of nanoparticle agglomerates ranging from tens to several hundreds of nanometers in size (Figure 2c).

To probe the cause of the observed instability of MPN **4** and to develop a ligand system capable of stabilizing these nanoparticles over long periods of time in both the solution and the solid state, a series of alkane alcohol ligands was prepared (Figure 3). In this series, ligands **5** and **6** contain more bulky alkane tail groups designed to prevent agglomeration of the nanoparticles in the solid state. To improve the stability of the ligand−nanoparticle core interaction, bidentate diols **7** and **8** were prepared with either one or two dodecyl groups.[22] This was done to separate the possible stabilization effects of increasing the strength of the nanoparticle core−ligand interaction from the effects of increasing steric bulk.

Derivatization of MPN **2** was again accomplished by stirring a toluene solution of the nanoparticle and a large excess of the desired ligand for 48 h at room temperature. In all cases, the nanoparticle could be precipitated from toluene using EtOH and then resuspended in toluene or $CHCl_3$. The stability of these derivatized nanoparticles was strongly dependent on the ligand: those functionalized with **5** and **6** rapidly precipitated from solution after they were resuspended but were stable for weeks in the solid state following their initial precipitation. Nanoparticles derivatized with **7** were stable for at least a month in solution, but were unstable if solvent was completely removed at any time after their initial precipitation from the derivatization reaction.[23] Nanoparticles derivatized with **8** proved to be the most stable: they were found to remain in solution for at least a month and were dispersible even after being dried in vacuo and stored in the solid state for a month (Figure 4).

The disparity in the observed stabilities of our alcohol-modified MPNs is the result of the alcohol structure and points to a loosely packed monolayer. Nanoparticles coated with dodecanol proved to be unstable in the solid state, whereas both monoalcohol ligands **5** and **6** are stable for long periods of time in the solid state. If the monolayer is sparsely packed, nanoparticles derivatized with **3** are able to approach close enough in the solid state that their cores can agglomerate, whereas the other two molecules present enough organic bulk at the surface to prevent agglomeration. In solution, however, these nanoparticles slowly precipitated over time, indicating a possible kinetic instability in the binding of the alcohol to the nanoparticle surface.[24] This was prevented in the case of ligands **7** and **8**, which are able to participate in bidentate binding to the nanoparticle surface. In monolayers formed from **7**, however, we observed instability in the solid state, indicating that the amount of organic coating was insufficient to prevent contact of the nanoparticle cores, thus allowing nanoparticle agglomeration. As ligand **8** was found to produce the most stable monolayer−nanoparticle system, we next characterized both MPN **9** and the reaction used to introduce the monolayer (Scheme 2).

Monolayer Characterization. Infrared (IR) spectroscopy was used to further characterize the monolayers of MPNs **2** and **9** (Figure 5). The IR spectrum of MPN **2** (Figure 5a) contained the expected methylene stretching peaks as well as a number of peaks in the fingerprint region (∼1500−1000 cm^{-1}) arising from

(22) For a recent example of the use of multivalent ligand−surface interactions to stabilize large gold nanoparticles, see: Stavens, K. B.; Pusztay, S. V.; Zou, S.; Andres, R. P.; Wei, A. *Langmuir* **1999**, *15*, 8337−8339.

(23) See Supporting Information for TEM micrographs of MPN **2** after derivitization with ligands **5**, **6**, and **7**.

(24) Kinetic instability in the binding of mono-alcohols **3**, **5**, and **6** to MPN **2** was verified by the observation that solutions of the modified nanoparticle could be stabilized against precipitation by the addition of excess free ligand; see Supporting Information for further details.

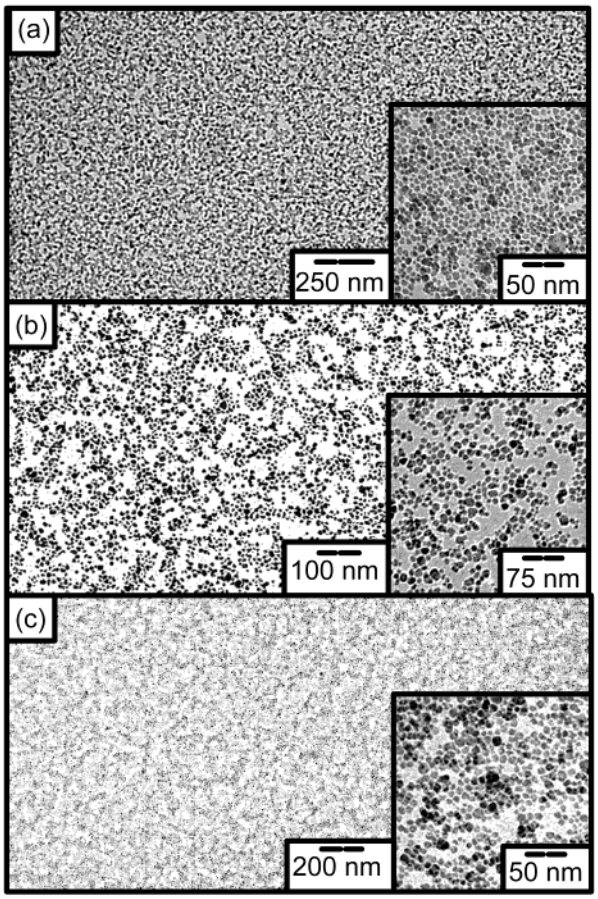

Figure 4. TEM micrographs of MPN **2** derivatized with diol ligand **8** (a) immediately after purification, (b) after 1 month in solution, and (c) redissolved after 1 month as a solid.

Scheme 2. Exchange of 8 into the Monolayer of MPN 2

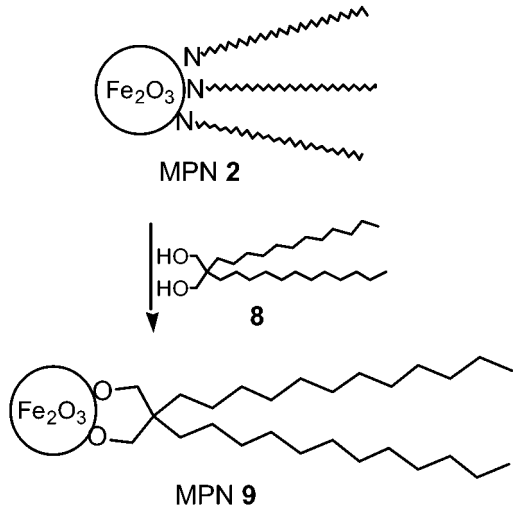

octylamine and trioctylamine, both of which are present during the formation of the nanoparticle.[25] A number of changes were observed after ligand displacement (Figure 5b), the most notable of which is the appearance of a strong adsorption at ca. 1050 cm^{-1} arising from C−O single-bond stretching.[26] Further, the CH_3/CH_2 stretching region (2700−2900 cm^{-1}) also showed an increase in intensity relative to the other spectral features, indicating an increase in the amount of long-chain hydrocarbons. Analysis of the peak positions in this region can yield information about the degree of order within the monolayer. Here, both MPN **2** and **9** exhibit peaks at ∼2954 cm^{-1} for $\nu_{as}(CH_3)$, ∼2926 cm^{-1} for $\nu_{as}(CH_2)$, and ∼2854 cm^{-1} for $\nu_s(CH_2)$ (inset of Figure 5b), indicating a disordered monolayer.[27] In both cases, an intense, broad adsorption at ∼550 cm^{-1} was observed, arising from the Fe_2O_3 core.[28]

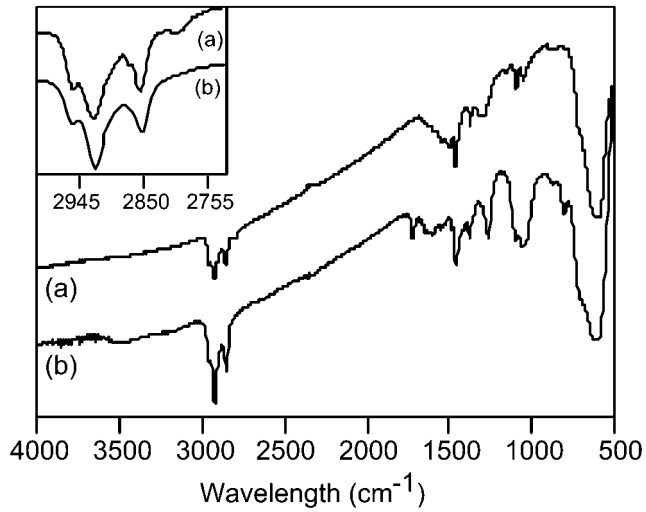

Figure 5. IR spectra (a) MPN **2** and (b) MPN **9**. Inset shows the methylene-stretching region in detail. Spectra were recorded as thin films cast from $CHCl_3$ solutions onto NaCl plates.

Thermal gravimetric analysis (TGA) and differential scanning calorimetry (DSC) were performed on MPNs **2** and **9** to further compare the two monolayers. The TGA trace of MPN **2** exhibits a steady decrease in mass throughout the range of the scan, with a final loss of 12% of the initial mass at 700 °C (Figure 6, solid trace). This mass loss is less than that observed for undeceneoate-coated MPNs (17.5% of the initial mass),[20] and it might indicate that the amine monolayer is somewhat less densely packed. For MPN **9**, a loss of 15% of the initial mass was observed over the same range (Figure 6, dashed trace).

DSC can be used to provide an estimate of the degree of monolayer order on the nanoparticles, as well-packed monolayers exhibit a "melting" transition from a crystalline-like to a liquidlike state on the nanoparticle surface. In previous agglomerate Fe_2O_3 nanoparticle−alkane thiol monolayer systems, this melting transition was observed at ∼10 °C for a dodecane thiol monolayer.[29] For both MPN **2** and **9**, DSC traces showed only a featureless, reversible curve between −100 and 200 °C (Figure 7), in good agreement with the IR data, which

(25) See Supporting Information for IR spectra of octylamine and trioctylamine. These data do not allow us to assign the chemical structure of the native monolayer, because the IR spectra of these molecules are nearly indistinguishable in this region. Further, the broad peak observed between 1600 and 1500 cm^{-1}, which neither octylamine nor trioctylamine exhibit, indicates that there might be other components of the native monolayer that are unknown at this time. Further, not all of these peaks disappear after monolayer displacement, indicating that some of the original functionality remains after exchange.

(26) A similar, strong stretch was also observed in the IR spectrum of **8**; see Supporting Information.

(27) *Thin Films*; Ulman, A., Ed.; Academic Press: Boston, 1999; Vol. 23.

(28) Nyquist, R. A.; Kagel, R. O. *Infrared Spectra of Inorganic Compounds* Academic Press: New York, 1971.

(29) Prozorov, T.; Gedanken, A. *Adv. Mater.* **1998**, *10*, 532−535.

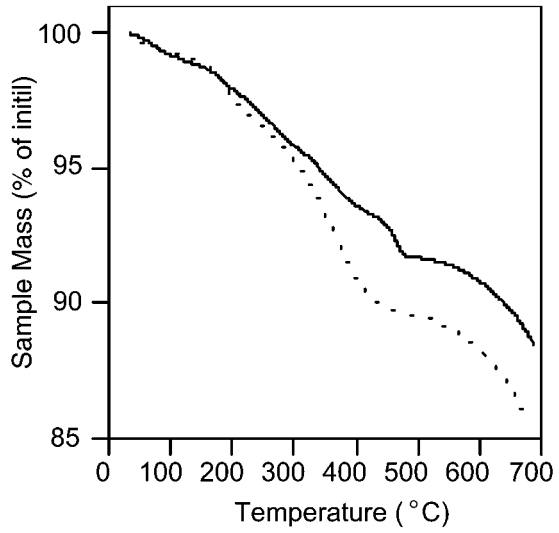

Figure 6. TGA results for (solid line) MPN **2** and (dashed line) MPN **9**. Heating rate = 10 °C/min, carrier gas = N_2.

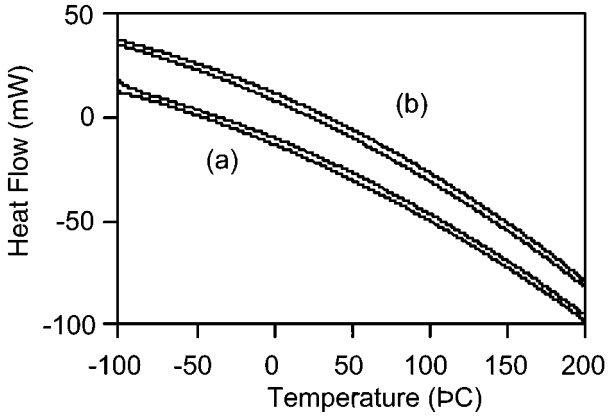

Figure 7. DSCs of (a) MPN **2** and (b) MPN **9**. Heating rate = 10 °C/min.

indicate a disordered monolayer. In sum, both the IR and TGA results confirm that we were able to modify the native monolayer of MPN **2** with diol **8**, and the DSC results indicate a less dense monolayer, suggested by the lack of a melting transition, than was observed for other Fe_2O_3 nanoparticle−organic monolayer systems.[30]

Characterization of the Nanoparticle Core. For some nanoparticle−monolayer systems, the properties of the inorganic core material can be affected by the type of attached ligand.[31] To determine whether any changes occurred the in core as a function of the monolayer, we next characterized both MPN **2** and **9** by electron paramagnetic resonance (EPR) and ultraviolet−visible (UV−vis) spectroscopy, as well as by powder X-ray diffraction (XRD).

The EPR spectra of both particles showed a broad, single transition at $g \approx 2$ with a line width of ~1800 G at room temperature, as is typical for nanoscopic Fe_2O_3 (Figure 8).[32,33] The UV−vis spectra of both MPN **2** and **9** (Figure 9) showed a broad absorbance, strong at short

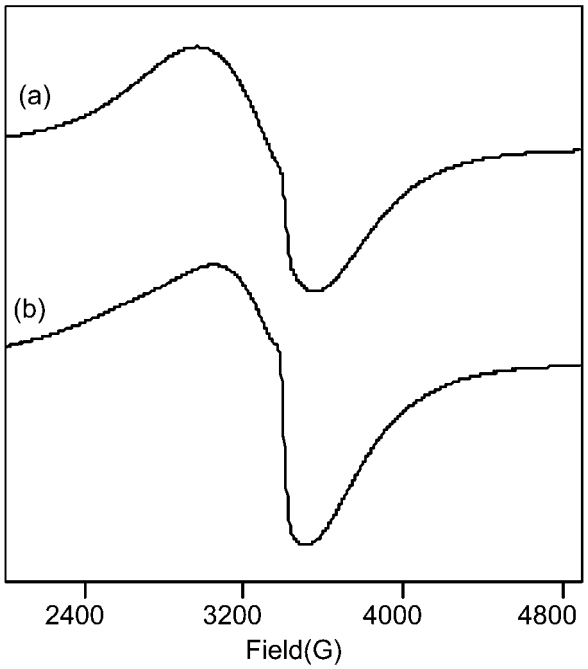

Figure 8. EPR spectra of (a) MPN **2** and (b) MPN **9**. Spectra were recorded as 5 mg/mL solutions of the nanoparticles in degassed $CHCl_3$.

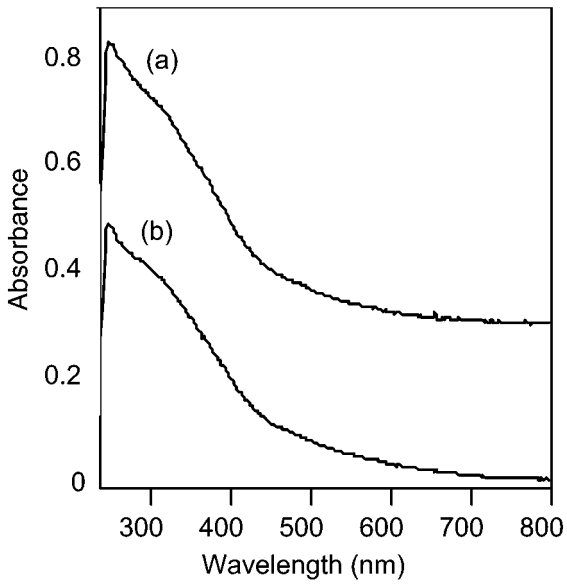

Figure 9. UV−vis spectra of (a) MPN **2** and (b) MPN **9**. Spectra were recorded as 0.1 mg/mL solutions of the nanoparticles in $CHCl_3$.

wavelengths and tailing out to long wavelengths, again typical for isolated Fe_2O_3 nanoparticles.[34] Finally, XRD of MPN **2** gave a diffraction pattern nearly identical to that observed by Alivisatos, with this pattern remaining unchanged for MPN **9** (Figure 10). In all cases, the lack of any significant change in the spectra obtained on both the amine- and alcohol-functionalized nanoparticles shows that the core functionality is unaffected by the nature of the monolayer.

Monolayer Modification Reactions. Optimization of the monolayer modification reaction of MPN **2** by **8**

(30) TGA and DSC data collected for MPNs modified with ligands **3**−**7** gave mass losses ranging from 12 to 22% of the intial mass and featureless DSC traces; see Supporting Information.

(31) Malinsky, M. D.; Kelly, L. K.; Schatz, G. C.; Van Duyne, R. P. *J. Am. Chem. Soc.* **2001**, *123*, 1471−1482.

(32) Cannas, C.; Gatteschi, D. Musinu, A.; Piccaluga, G.; Sangregorio, C. *J. Phys. Chem. B* **1998**, *102*, 7721−7726.

(33) In both cases, no second signal at $g \approx 4.3$ appeared, which indicates the lack of rhombic Fe^{3+} sites that are sometimes observed for nanoscopic Fe_2O_3.

(34) Sohn, B. H.; Cohen, R. E. *Chem. Mater.* **1997**, *9*, 264−269.

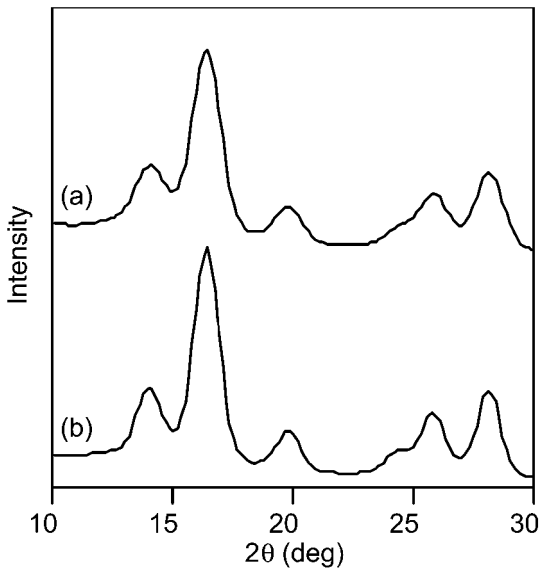

Figure 10. Powder XRD patterns (Mo Kα radiation) of (a) MPN **2** and (b) MPN **9**.

Table 1. Conditions Used for Exchange Reactions[a]

entry	**8** (mg)	temp (°C)	C−O/Fe−O ratio[b]
1	3	25	0.13
2	10	25	0.18
3	30	25	0.23
4	60	25	0.25
5	3	50	0.14
6	10	50	0.37
7	20	50	0.36

[a] All reactions were carried out with 30 mg of MPN **2**.[35] [b] Intensity ratio of the alcohol C−O to MPN Fe−O stretch.

was next carried out. Here, we explored changes in the ratio between the two reactants as well as the reaction temperature (Table 1). The resulting nanoparticles were characterized by IR spectroscopy, where the degree of derivatization can be estimated by the relative strengths of the C−O and Fe−O stretches (Table 1). Room-temperature reactions were found to inefficiently incorporate **8** into the monolayer of MPN **2**, even when a large excess of **8** was used in the reaction (Table 1, entries 1−4). At 50 °C, however, significantly less ligand was needed to achieve a higher degree of surface derivatization (Table 1, entries 5−7), and an MPN **2**/**8** mass ratio of at least 3:1 was found to produce a highly modified monolayer.

As mixed-monolayer systems are often used to impart complex functionality into monolayer−nanoparticle systems, we next explored the simultaneous introduction of multiple alcohol ligands into the monolayer of MPN **2**.[36] Here, both **8** and an amide-functionalized derivative, **10**, were stirred in different ratios with MPN **2** (Scheme 3 and Table 2) using the previously described conditions. The resulting nanoparticles, MPN **11**, were then purified by multiple toluene/ethanol precipitations and were then characterized by IR spectroscopy (Figure 11). In addition to the C−O stretching, which arises

Scheme 3. Simultaneous Exchange of Ligands 8 and 10 into the Monolayer of MPN 3 to Yield MPN 12

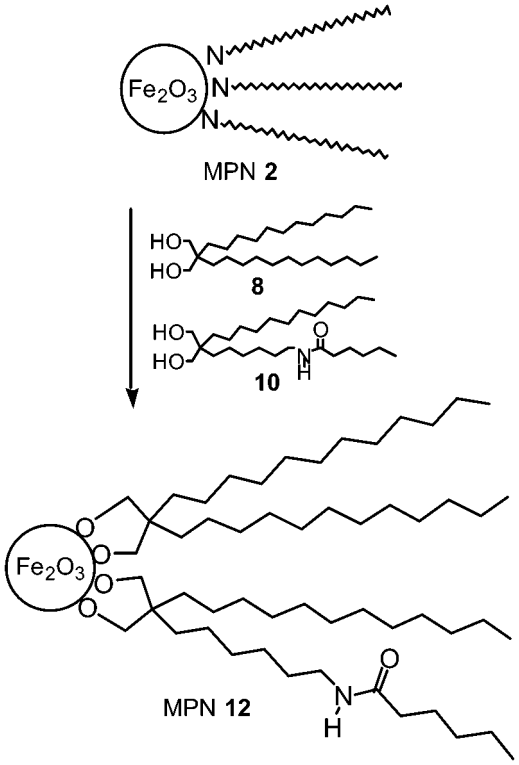

Table 2. Amounts of MPN 2 and Free Ligands Used for Simultaneous Monolayer Modification of MPN 2 with Ligands 8 and 10[a]

entry	MPN **2** (mg)	**8** (mg)	**10** (mg)	C═O/C−O ratio[b]
1	30	4	16	0.76
2	30	8	12	0.67
3	30	12	8	0.40

[a] Reactions were run and purified as described above. [b] Intensity ratio of the amide C═O to alcohol C−O stretch.

from both **8** and **10**, a new peak at ∼1637 cm^{-1} arising from the amide C═O stretch is also observed for MPN **11**.[37] As expected, as the ratio of **10** to **8** was increased, the relative intensity of the amide C═O stretch increased as compared to the C−O stretch, because of the relative increase of **10** in the monolayer. This indicates that it is possible to define the relative surface coverage of the two ligands by the synthetic conditions.

Conclusions

In summary, we have developed a divergent synthetic pathway that allows access to mixed monolayer-protected γ-Fe_2O_3 nanoparticles. We found that alkane alcohols can be introduced into the monolayer by stirring amine-coated nanoparticles in solution with the desired alcohol. Here, it was found that both kinetic stabilization, in the form of multivalent ligand−nanoparticle core contacts, and steric stabilization, in the form of a bulky tail group, were necessary to prevent nanoparticle agglomeration. The relative instability of

(35) All reactions were carried out using 20 mL of a 1:1 mixture of toluene and $CHCl_3$, and all products were purified by precipitation with MeOH, followed by extensive MeOH washings. Full spectra of these nanoparticles are given in the Supporting Information.

(36) A stepwise reaction was also explored, but it was found to give unreliable results. See Supporting Information.

(37) This peak is insignificantly shifted from the free ligand (∼1640 cm^{-1}) and indicates that the amide group is not involved in binding to the nanoparticle surface.

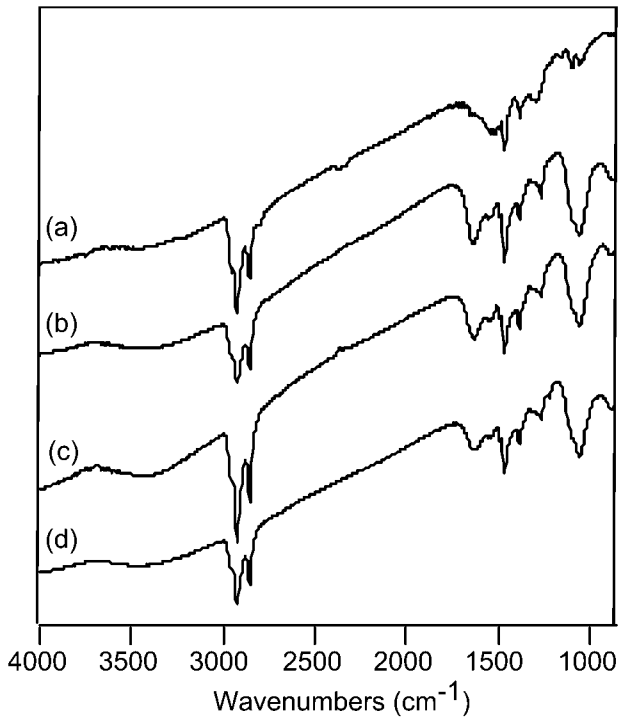

Figure 11. IR spectra from simultaneous exchange study. Spectra are for (a) MPN **2** and (b−d) entries 1−3, respectively, of Table 2. All spectra were recorded as thin films cast from $CHCl_3$ onto NaCl plates.

the nanoparticle monolayer might arise from the sparse monolayer packing observed in these systems, as inferred from TGA, DSC, and IR studies on MPNs **2** and **9**. The nature of the γ-Fe_2O_3 core is unaffected by changes in the ligand shell; EPR, UV−vis, and powder XRD spectra are unchanged for nanoparticles with either their native amine monolayers or modified alcohol monolayers. This reaction was optimized to maximize the inclusion of the incoming ligand by using a 3:2 MPN **2**-to-ligand mass ratio and conducting the reaction at 50 °C. Finally, we explored the creation of monolayer systems made from two molecular components and found that the most reliable method for introducing multiple functionalities in a predetermined ratio is to exchange in the two components simultaneously. Currently, we are using this ligand design and displacement reaction for the creation of recognition-element-functionalized MPNs to explore their potential application as components in magnetic materials and as biological probes.

Experimental Section

General. Unless otherwise noted, all reactions were carried out in oven-dried glassware under an argon atmosphere. Toluene and CH_2Cl_2 were distilled over CaH_2 under argon. THF was distilled over sodium/benzophenone ketyl immediately before use. ^1H NMR spectra were recorded in $CDCl_3$ (Cambridge Isotope Labs, Inc.) at 200 MHz and referenced internally to TMS at 0.0 ppm. All reagents and other solvents were used as received from commercial sources. IR spectra were recorded on a Perkin-Elmer 783 spectrometer. Samples were prepared by drop casting concentrated CH_2Cl_2 or $CHCl_3$ analyte solutions onto NaCl plates. UV−vis samples were prepared as $CHCl_3$ solutions, and a 1-cm-path length quartz cell was used. EPR spectra were recorded on an IBM ESP-300 X-band spectrometer. TEM micrographs were obtained on a JEOL-100CX electron microscope operating at 100 keV. Samples were prepared by dropping $CHCl_3$ solutions of the desired nanoparticles onto 300-mesh Cu grids coated with a carbon film. TGA was performed on a TA Instruments TGA 2050 apparatus. DSC was obtained on a Perkin-Elmer Pyris 1 instrument. XRD patterns were recorded on a Nonius instrument with a KappaCCD area detector at room temperature using graphite-monochromated Mo Kα radiation.

Scheme 4. Synthesis of Ligands 7 and 8

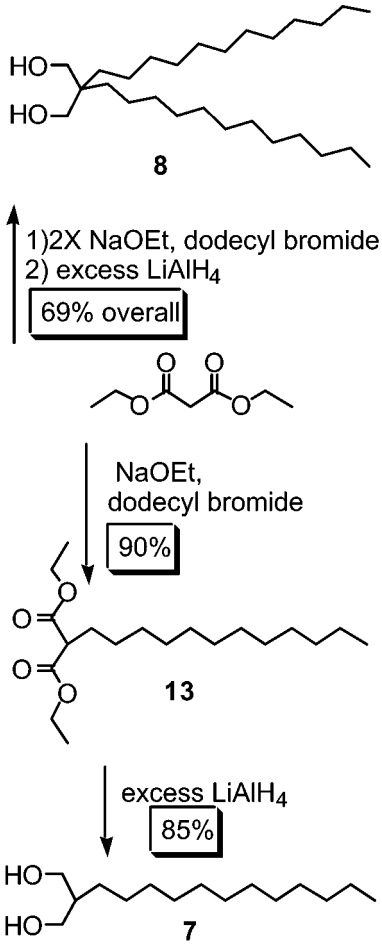

13,13-Bis-hydroxymethylpentacosane (8) (Scheme 4). In a 250-mL three-neck round-bottom flask, diethyl malonate (2.5 g, 15.6 mmol, 2.4 mL) was dissolved in 100 mL of absolute EtOH, giving a clear solution. NaOEt (19 mmol, 8.1 mL of a 21 wt % solution in EtOH) was then added slowly, and the reaction mixture became bright orange. After the mixture had been for 30 min, dodecyl bromide (5.85 g, 23.4 mmol, 5.7 mL) was added, and the reaction mixture was refluxed for 48 h, during which time a white precipitate formed. After the reaction mixture had been cooled to room temperature, a second equal portion of NaOEt was added, followed by 30 min of stirring at room temperature, the addition of a second equal amount of dodecyl bromide, and another 48 h at reflux. The EtOH was removed in vacuo, and the resulting thick slurry was dissolved in EtOAc. The organic fraction was washed once with each 1 M aqueous HCl and saturated aqueous NaCl and dried over $MgSO_4$. Solvent removal gave a clear oil, which was filtered through SiO_2 with 10% EtOAc/hexanes and used without further purification (6.5 g, 84% yield).

In a 100-mL round-bottom flask, the product from the preceding reaction (2.0 g, 4.02 mmol) was dissolved in 40 mL of THF and cooled to −78 °C. Lithium aluminum hydride (24 mmol, 24 mL of a 1 M solution in THF) was then added dropwise, and the reaction mixture was stirred overnight at room temperature. After careful quenching of the reaction by the dropwise addition of H_2O, the reaction mixture was

transferred to a separatory funnel, washed once with each 1 M aqueous NaOH and saturated aqueous NaCl, and dried over $MgSO_4$. Solvent removal resulted in an off-white solid, which was chromatographed (SiO_2 gradient elution, EtOAc to 10% MeOH/EtOAc) to yield the product as a white solid (1.4 g, 82% yield). ^{1}H NMR ($CDCl_3$, 200 MHz): δ (ppm) ~3.7 (m, 2H), 3.57 (d, 4H, J = 5.4 Hz), 2.11 (m, 2H), 1.26 (m, 40H), 0.88 (m, 6H). IR (thin film from CH_2Cl_2 on NaCl plate): ν_{max} 3340, 2915, 2820, 1460, 1020 cm^{-1}. Anal. Calcd. for $C_{27}H_{56}O_2$: C, 78.57; H, 13.68. Found: C, 77.93; H, 13.41.

Diethyl Dodecylmalonate (14). In a 250-mL three-neck round-bottom flask, diethyl malonate (16 g, 100 mmol, 15.2 mL) was dissolved in 100 mL of absolute EtOH, giving a clear solution. NaOEt (100 mmol, 42 mL of a 21 wt % solution in EtOH) was then added slowly, and the reaction mixture became bright orange. After the mixture had been stirred for 30 min, dodecyl bromide (5.0 g, 20 mmol, 4.8 mL) was added, and the reaction mixture was refluxed for 48 h, during which time a white precipitate formed. The EtOH was removed in vacuo, and the resulting thick slurry was dissolved in EtOAc. The organic fraction was washed once with each 1 M aqueous HCl and saturated aqueous NaCl and dried over $MgSO_4$. Solvent removal gave a thick yellow/orange oil, which was chromatographed (SiO_2/hexanes) to give the product as a colorless oil (6.0 g, 90% yield). ^{1}H NMR ($CDCl_3$, 200 MHz): δ (ppm) 4.19 (q, 4H, J = 6.88 Hz), 3.31 (t, 1H, J = 7.88 Hz), 1.88 (m, 2H), 1.25 (m, 20H), 0.88 (t, 3H, J = 6.0 Hz). IR (thin film from CH_2Cl_2 on NaCl plate): ν_{max} 2915, 2810, 1735, 1720, 1460, 1150, 1015 cm^{-1}. Anal. Calcd. for $C_{19}H_{36}O_4$: C, 69.47; H, 11.05. Found: C, 69.59; H, 11.25.

2-Hydroxymethyltetradecan-1-ol (7) (Scheme 4). In a 100-mL round-bottom flask, **13** (500 mg, 1.5 mmol) was dissolved in 20 mL of THF and cooled to −78 °C. Lithium aluminum hydride (9 mmol, 9 mL of a 1 M solution in THF) was then added dropwise, and the reaction mixture was allowed to stir overnight at room temperature. After careful quenching of the reaction by the dropwise addition of H_2O, the reaction mixture was transferred to a sepratory funnel, washed once with each 1 M aqueous NaOH and saturated aqueous NaCl, and dried over $MgSO_4$. Solvent removal gave the product as an off-white solid, which was chromatographed (SiO_2 gradient elution, EtOAc to 10% MeOH/EtOAc) to yield the product as a white solid (310 mg, 85% yield). ^{1}H NMR ($CDCl_3$, 200 MHz): δ (ppm) ~3.7 (m, 4H), 2.15 (t, 2H, J = 4.9 Hz), 1.77 (m, 1H), 1.26 (m, 20H), 0.88 (m, 3H). IR (thin film from CH_2Cl_2 on NaCl plate): ν_{max} 3290, 2910, 2815, 1490, 1010, 680 cm^{-1}. Anal. Calcd. for $C_{15}H_{32}O_2$: C, 73.71; H, 13.20. Found: C, 73.88; H, 13.35.

13-Dodecylpentacosane-13-ol (5) (Scheme 5). In a 100-mL round-bottom flask, dimethyl carbonate (450 mg, 5.0 mmol, 0.42 mL) was dissolved in 10 mL of THF and cooled to −78 °C. Dodecylmagnesiumbromide (20 mmol, 20 mL of a 1 M solution) was then added, and the reaction mixture was allowed to stir for three nights at room temperature. The reaction was quenched by the addition of MeOH and then saturated aqueous NH_4Cl. The organic phase was transferred to a separatory funnel, washed once with a saturated aqueous NaCl solution, and dried over $MgSO_4$. After solvent removal, the crude material was recrystallized from EtOAc to yield the product as a white solid (2.2 g, 84% yield).^{1}H NMR ($CDCl_3$, 200 MHz): δ (ppm) ~3.6 (m, 1H), 1.26 (m, 66H), 0.88 (m, 9H). IR (thin film from CH_2Cl_2 on NaCl plate): ν_{max} 3370, 2910, 2820, 1480 cm^{-1}. Anal. Calcd. for $C_{37}H_{76}O$: C, 82.76; H, 14.27. Found: C, 82.57; H, 14.46.

Pentacosane-13-ol (6) (Scheme 5). In a 100-mL round-bottom flask, ethyl formate (500 mg, 6.67 mmol, 0.54 mL) was dissolved in 10 mL of THF and cooled to −78 °C. Dodecylmagnesium bromide (20 mmol, 20 mL of a 1 M solution) was then added and the reaction mixture was allowed to stir for three nights at room temperature. The reaction was quenched by the addition of MeOH and then saturated aqueous NH_4Cl. The organic phase was transferred to a separatory funnel, washed once with a saturated aqueous NaCl solution, and dried over $MgSO_4$. After solvent removal, the crude material was recrystalized from EtOAc to yield the product as a white solid (2.1 g, 84% yield).^{1}H NMR ($CDCl_3$, 200 MHz): δ (ppm) 3.58 (m, 1H), 1.29 (m, 44H), 0.88 (m, 6H). IR (thin film from CH_2Cl_2 on NaCl plate): ν_{max} 3310, 3190, 3070, 2915, 2810, 1270, 770 cm^{-1}. Anal. Calcd. for $C_{25}H_{52}O$: C, 81.44; H, 14.22. Found: C, 81.38; H, 14.20.

Scheme 5. Synthesis of Ligands 5 and 6

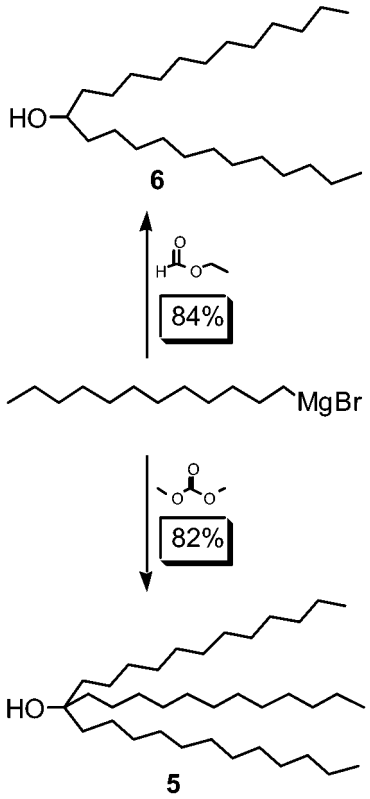

Diethyl 5-Cyanopentyl Dodecyl Malonate (16). In a 125-mL three-neck round-bottom flask, **14** (7.0 g, 21 mmol) was dissolved in 30 mL of THF and cooled to −78 °C. Lithium di-*iso*-propyl amide (24 mmol, 24 mL of a 1 M THF solution) was then added and the reaction mixture was subsequently allowed to stir for an hour at room temperature. 6-Bromohexane nitrile (6.0 g, 25 mmol, 3.5 mL) was then added, and the reaction mixture was refluxed for 36 h under argon, during which time a precipitate formed. After the reaction had been by the careful addition of MeOH, the organic fraction was washed once with each 1 M aqueous HCl and saturated aqueous NaCl, and dried over $MgSO_4$. Solvent removal gave a thick orange oil, which was chromatographed (SiO_2 gradient elution of hexanes to 10% EtOAc/hexanes) to give the product as a pale yellow oil (7.4 g, 85% yield). ^{1}H NMR ($CDCl_3$, 200 MHz): δ (ppm) 4.18 (q, 4H, J = 6.88 Hz), 2.33 (t, 2H, J = 6.9 Hz), 1.89 (m, 4H), ~1.5 (mm, 4H), 1.25 (m, 22H), 0.88 (t, 3H, J = 6.8 Hz). IR (thin film from CH_2Cl_2 on NaCl plate): ν_{max} 2920, 2840, 2245, 1620, 1480, 1020 cm^{-1}. Anal. Calcd. for $C_{25}H_{45}NO_4$: C, 70.88; H, 10.71. Found: C, 70.84; H, 10.95.

1-Amino-7,7-bis-hydroxymethylnonadecane (17). In a 100-mL round-bottom flask, **15** (500 mg, 0.95 mmol) was dissolved in 20 mL of THF and cooled to −78 °C. Lithium aluminum hydride (10 mmol, 10 mL of a 1 M solution in THF) was then added dropwise, and the reaction mixture was allowed to stir overnight at room temperature. After careful quenching of the reaction by the dropwise addition of H_2O, the reaction mixture was transferred to a separatory funnel, washed once with each 1 M aqueous NaOH and saturated aqueous NaCl, and dried over $MgSO_4$. Solvent removal gave viscous yellow oil, which was used without further purification in the next reaction (310 mg, 95% yield). ^{1}H NMR ($CDCl_3$, 200 MHz): δ (ppm) 3.55(s, 4H), 2.69 (t, 2H, J = 6.91 Hz), 2.25 (bs,

Scheme 6. Synthesis of Ligand 10

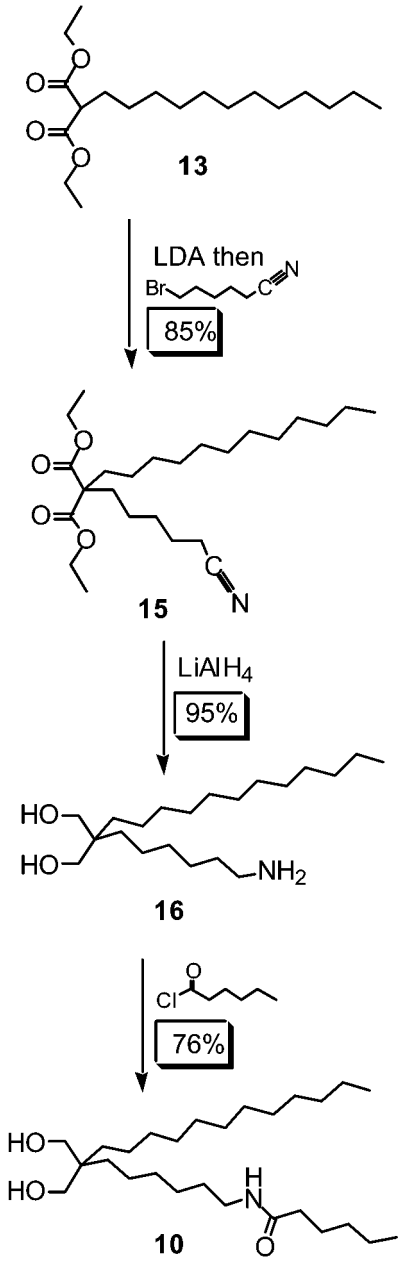

2H), 1.29 (m, 32H), 0.88 (t, 3H, $J = 6.8$ Hz). IR (thin film from CH_2Cl_2 on NaCl plate): ν_{max} 3360, 3280, 2920, 2845, 1460, 1030 cm^{-1}.

***N*-Hexanoyl-1-amino-7,7-bis-hydroxymethylnonadecane (10) (Scheme 6).** In a 50-mL round-bottom flask, **16** (310 mg, 0.9 mmol) was dissolved in 25 mL of CH_2Cl_2. Triethylamine (200 mg, 1.9 mmol, 0.27 mL) was added, and the light yellow solution was cooled to −78 °C. Hexanoyl chloride (100 mg, 0.76 mmol, 0.1 mL) was added dropwise, and the reaction mixture was allowed to stir for 3 h at room temperature. The mixture was then washed once with each 1 M aqueous HCl saturated aqueous $NaHCO_3$, and saturated aqueous NaCl before being dried over $MgSO_4$. Solvent removal gave a white tacky solid, which was chromatographed (SiO_2 gradient elution, 1:1 EtOAc/hexanes to 5% MeOH/EtOAc) to give the product as a thick, colorless oil (250 mg, 76% yield). ^1H NMR ($CDCl_3$, 200 MHz): δ (ppm) 5.43 (bs, 1H), 3.57 (s, 4H), 3.24 (q, 2H, $J = 8.32$ Hz), 2.34 (m, 2H), 2.15 (t, 2H, $J = 7.86$ Hz), ~1.5 (mm, 4H), 1.26 (m, 34H), 0.89 (m, 6H). IR (thin film from CH_2Cl_2 on NaCl plate): ν_{max} 3300, 3090, 2920, 2845, 1640, 1550, 1470, 1030 cm^{-1}. Anal. Calcd. for $C_{27}H_{55}NO_2$: C, 73.41; H, 12.55;N, 3.17. Found: C, 73.68; H, 12.75; N, 3.25.

Representative Nanoparticle Monolayer Modification Reaction. In a 50-mL round-bottom flask, MPNs **2** (150 mg) and **8** (100 mg) were dissolved in 25 mL of a 1:1 mixture of $CHCl_3$ and toluene.[38] The flask was fitted with an air condenser, and the dark red/brown solution was stirred for two nights at 50 °C under argon. After the reaction mixture had been cooled to room temperature, the solvents were removed, and the resulting glassy brown solid dissolved in the minimum amount of toluene necessary (typically 10−20 mL) and precipitated with MeOH. This procedure was then repeated as needed to remove unattached ligands fully, as monitored by TLC.

Acknowledgment. This research was supported by the National Science Foundation (CHE-9905492 and MRSEC instrumentation) and the National Institutes of Health (GM 62998). V.M.R. acknowledges support from the Alfred P. Sloan Foundation, Research Corporation, and the Camille and Henry Dreyfus Foundation. A.K.B. thanks the American Chemical Society, Division of Organic Chemistry and Boehringer Ingelheim Pharmaceuticals, Inc. for receipt of a 2000-2001 Graduate Fellowship. We thank the X-ray Structural Characterization Facility at the UMass Chemistry Department (NSF Grant CHE-9974648) and Dr. A. Chandrasekaran for collection of the XRD data. The Penelle Group (UMass Department of Polymer Science and Engineering) is thanked for assistance in the acquisition of TGA and DSC data.

Supporting Information Available: Additional characterization (TEM, DSC, TGA) of MPNs and spectra of intermediates (PDF). This material is available free of charge via the Internet at http://pubs.acs.org.

CM011689P

(38) We found that distilled solvents were not required for displacement reactions.